ACS OMEGA

http://pubs.acs.org/journal/acsodf

Article

In Vitro Identification of Potential Metabolites of Plinabulin (NPI 2358) in Hepatic Preparations Using Liquid Chromatography–Ion Trap Mass Spectrometry

Nasser S. Al-Shakliah,* Adnan A. Kadi, Rashad Al-Salahi, and A. F. M. Motiur Rahman

Cite This: *ACS Omega* 2022, 7, 21465–21472

Read Online

ACCESS | Metrics & More | Article Recommendations

ABSTRACT: Plinabulin (**1**, NPI2358), a vascular disrupting agent (VDA) molecule, is a synthetic analogue of the natural product phenylahistin (**2**, NPI 2350), which is isolated from *Aspergillus ustus*. Evaluation of the *in vitro* metabolic profile of VDA plinabulin using human liver microsomes (HLMs) and HepaRG Cells Cryopreserved is described. HLMs and HepaRG Cells Cryopreserved were prepared in-house and incubated with plinabulin according to published methodologies. The incubated mixtures were analyzed by liquid chromatography–ion trap mass spectrometry to identify possible metabolic products. The incubated plinabulin (**1**) revealed the presence of several peaks representing 19 tentative metabolites in HLMs and HepaRG Cells Cryopreserved in the presence of NADPH (nicotinamide adenine dinucleotide phosphate) and in the absence of NADPH-generating system, respectively. However, in NADPH absence, no metabolites and microsomes were generated for **1** in incubated HLMs, indicating a likely involvement of CYP450 enzymes in the metabolism. The metabolite structures, obtained from HLMs and HepaRG Cells Cryopreserved incubations, were elucidated by LC–MS/MS fragmentation study. Seventeen phase-I metabolites were proposed to be the results of isomerization, hydroxylation, hydration, and oxygenation of **1** in HLMs and two isomeric phase-II sulfate conjugate metabolites of **1** in HepaRG Cells Cryopreserved incubation.

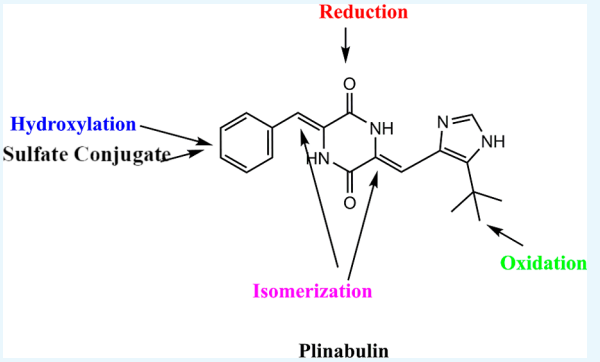

1. INTRODUCTION

Plinabulin (**1**, NPI2358) has been found as a potent vascular disrupting agent (VDA) against tubulin depolymerization and is currently being used in phase III clinical trial for non-small cell lung cancer (NSCLC) therapy.[1,2] Plinabulin as a new drug application in combination with granulocyte colony-stimulating factor for chemotherapy-induced neutropenia prevention has been approved by FDA.[3] Plinabulin enhanced the docetaxel antitumor activity positively with a favorable safety profile, as indicated by results with NSCLC patients,[4] and provided significant clinical benefit to patients with solid tumors as well. According to World Health Organization reports, lung cancer is the most common malignant disease worldwide and is the main cause of death from cancer (estimated to be 901,746 new cases each year), particularly among men.[5] From the data estimated in 2008, among the 16,632 cases diagnosed with lung cancer in the Arab league world, 13,826 cases (79.7%) were males and 2806 (20.3%) were females, and this study predicts that there will be 29,576 new cases in 2020.[6] After reviewing the previous literature reviews that were related to plinabulin, we did not find any study on plinabulin metabolism. During the drug discovery process, various issues with respect to pharmacodynamics, pharmacokinetics, and toxicity are commonly encountered. Drug metabolism is a major criterion in the high-throughput screening of prospective drugs. Hence, the nature of the metabolites produced from the drug must be thoroughly studied. Studying *in vitro* drug metabolism can be useful in the design of clinical studies, particularly those that examine drug–drug interactions. Previously reported studies on plinabulin were focused only on its synthesis, activity, and clinical trial development, and no research was carried out to identify its metabolites. *In vitro* metabolism should provide data that closely match that acquired from whole animal investigations because the compounds will be in the early phases of development; therefore, the present study was aimed to carry out the *in vitro* identification and characterization of plinabulin potential metabolites in hepatic preparations using the liquid chromatography–ion trap mass spectrometry (LC-ITMS/MS) technique. Employing human liver microsomes (HLMs) and HepaRG

Received: February 15, 2022
Accepted: June 1, 2022
Published: June 14, 2022

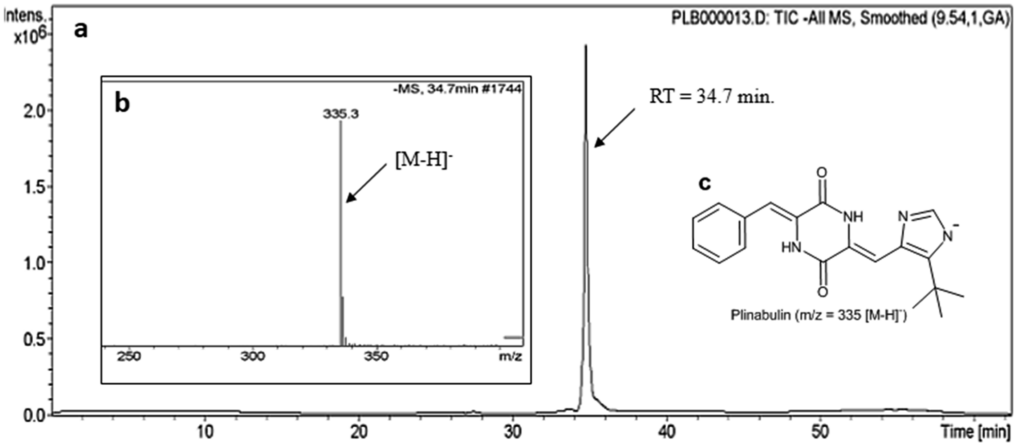

Figure 1. (a) TIC of **1**; (b) MS spectra of **1**; (c) chemical structure of **1**.

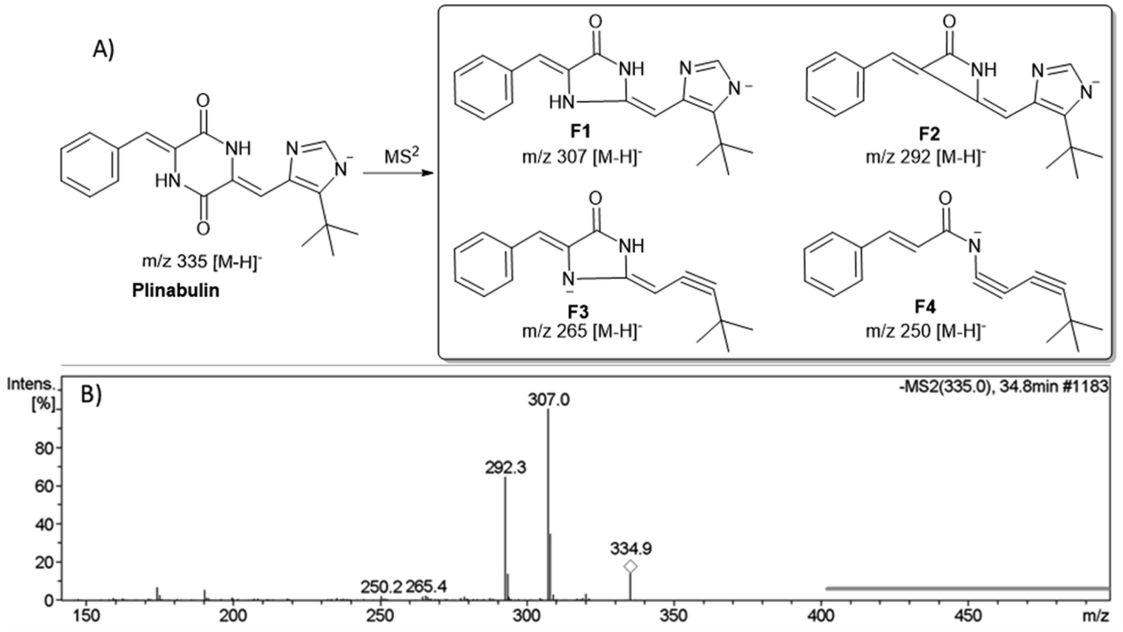

Figure 2. (A) Proposed chemical structrure of **1** and its MS/MS spectrum. (B) MS/MS spectrum ions of **1**

Cells Cryopreserved, the *in vitro* metabolic profile of **1** was studied. Thus, 19 proposed metabolites resulted from five main reactions including isomerization, oxidation, reduction, hydration, and conjugation. Among them, 17 were produced by HLMs, while the last 2 were by HepaRG Cells Cryopreserved. The presence of two geometric centers ($E-Z$) in the structure of **1** led to the formation of several isomer metabolites, which is considered a remarkable phenomenon and worthy of study. The E to Z geometrical isomers are considered the main metabolic pathway of **1** metabolites. Four proposed geometrical isomers (*EE*, *EZ*, *ZE*, and *ZZ*) were detected after incubation of the parent drug with HLMs and HepaRG Cells Cryopreserved. These had different retention times with the same m/z and the same MS/MS spectra of the parent compound.

2. MATERIALS AND METHODS

2.1. Chemicals and Reagents. Water was obtained from Milli-Q connected to an Elix Millipore water purification system (Millipore, USA). Acetonitrile HPLC grade, ammonium formate, and magnesium chloride were obtained from BDH laboratory supplies (Poole-UK). Nicotinamide adenine dinucleotide phosphate (NADPH) reduced form were obtained from ACROS, USA. Plinabulin (NPI2358) was obtained from Selleck Chemicals, USA. Pooled male human liver microsomes (M0567) were purchased from Sigma-Aldrich company (West Chester, PA, USA). The protein content of HLMs was 20 mg/mL protein in 250 mM sucrose. HepaRG Cells Cryopreserved (HPRGC10) were purchased from ThermoFisher company (Waltham, MA USA).

2.2. *In Vitro* Studies. *2.2.1. HLM Incubations.* At pH = 7.4, plinabulin (30 μM) in dimethyl sulfoxide was added to the phosphate buffer (0.08 M) with HLMs and stirred for 5 min at 37 °C for equilibration in water bath. The NADPH solution (1 mM) and microsomal protein (1 mg/mL) were added to start the incubation process (total volume of incubation mixture was 1 mL). NAPDH was replaced with water or microsomal protein to prepare the controls. After incubation (90 min), ice-cold acetonitrile (2 mL) was added to precipitate the proteins. At 14,000 rpm, the sample was centrifuged (10 min), and the supernatant was transferred to a fresh container and then evaporated under a stream of nitrogen. The reconstituted residue was transferred into a HPLC vial for analysis.

https://doi.org/10.1021/acsomega.2c00929
ACS Omega 2022, 7, 21465−21472

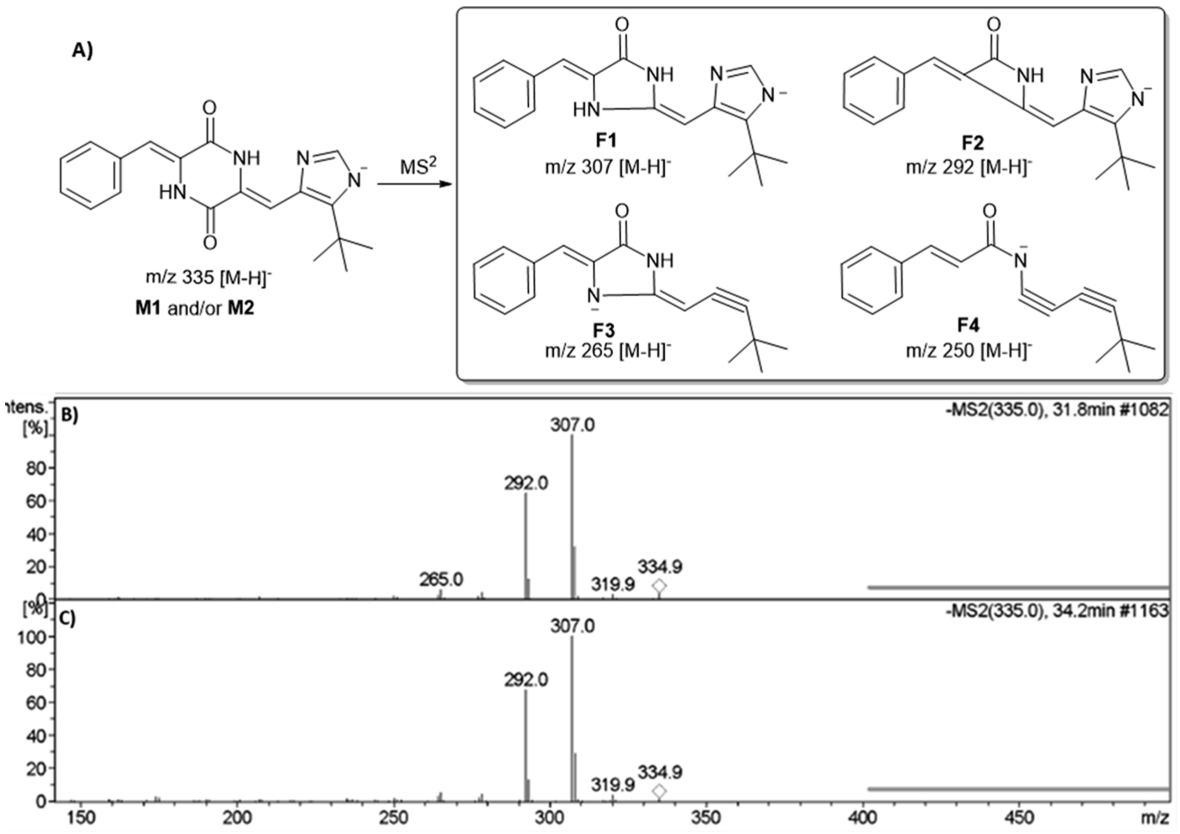

Figure 3. (A) Proposed chemical structure of **M1**/**M2** and their MS/MS fragments; (B) MS/MS spectrum of **M1**; (C) MS/MS spectrum of **M2**.

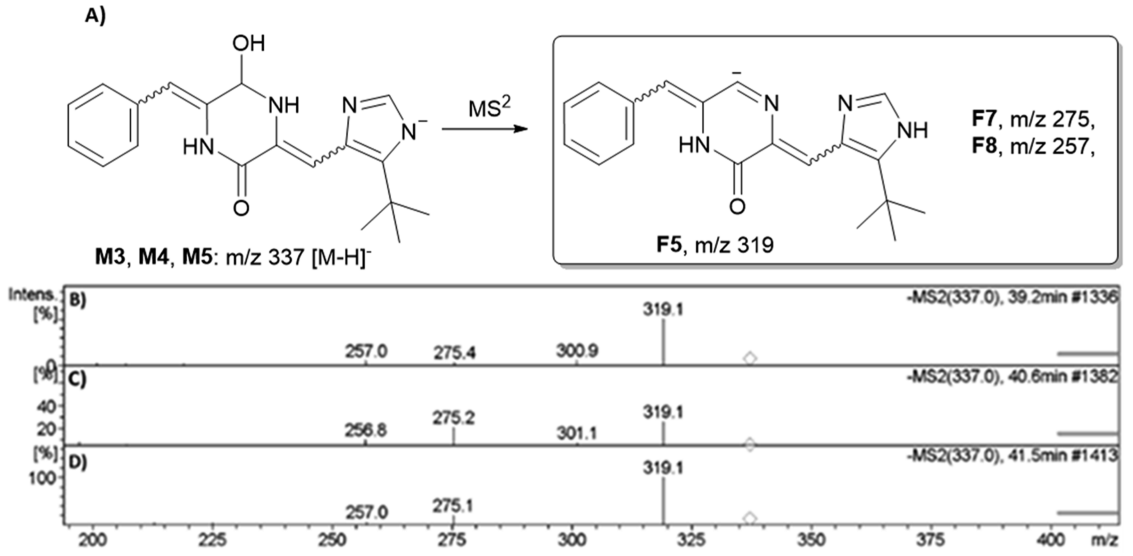

Figure 4. (A) Proposed chemical structure of **M3**, **M4**, and **M5** and their most abundant MS/MS fragments; (B) MS/MS spectrum of **M3**; (C) MS/MS spectrum of **M4**; D) MS/MS spectrum of **M5**.

2.2.2. Incubation of Plinabulin with HepaRG Cells Cryopreserved. The cell suspensions were preincubated at 37 °C for 10 min, and then 2 mL of this suspension was added to the appropriate container at room temperature (RT) except for the control container. The incubation was initiated by adding 2 μl of a 5mM stock solution of **1**. After incubation of the samples (2 h), ice-cold acetonitrile (2 mL) was added to precipitate the proteins. At 14,000 rpm, the sample was centrifuged (10 min), and the supernatant was collected in a fresh container and then evaporated under a stream of nitrogen. The reconstituted residue was transferred into a HPLC vial for analysis. All experiments were duplicated.

2.3. Chromatographic Conditions. Employing an Agilent 1200 series system containing of G1311A quaternary pump, a G1322A degasser, a G1367B HIP-ALS autosampler, a G1316A thermostatted column compartment, and a G1315B DAD detector, the separation was performed. An eclipse plus C18 (4.6 × 150 mm 3.5 μm) column and a mobile phase composed of 5

https://doi.org/10.1021/acsomega.2c00929
ACS Omega 2022, 7, 21465−21472

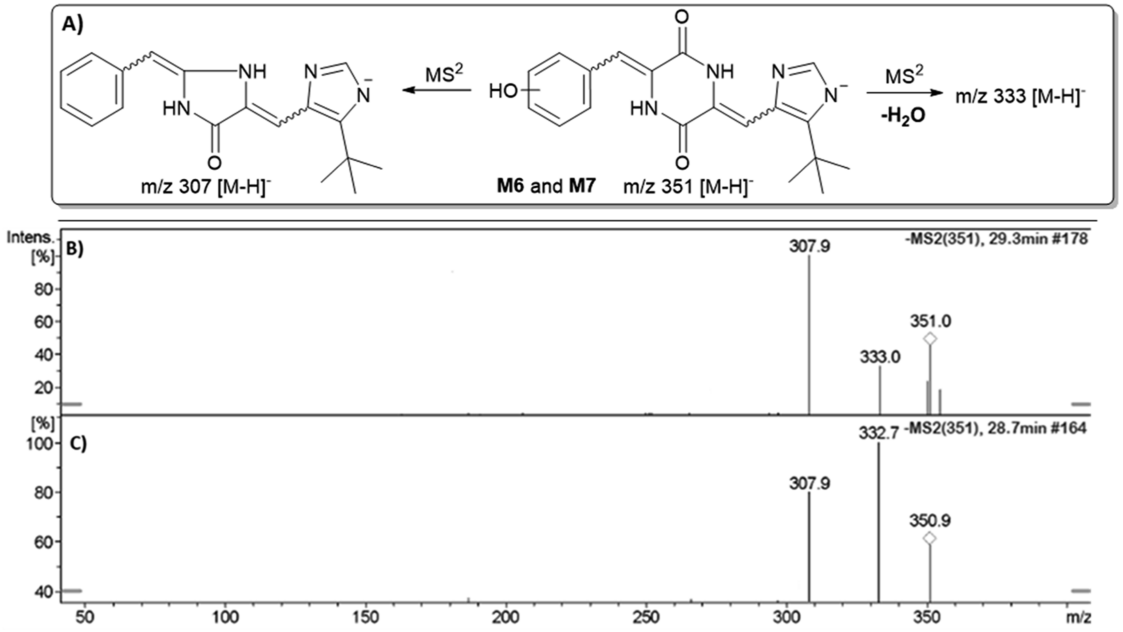

Figure 5. (A) Proposed chemical structure of **M6** and **M7** and their most abundant MS/MS fragments; (B) MS/MS spectrum of **M6**; (C) MS/MS spectrum of **M7**.

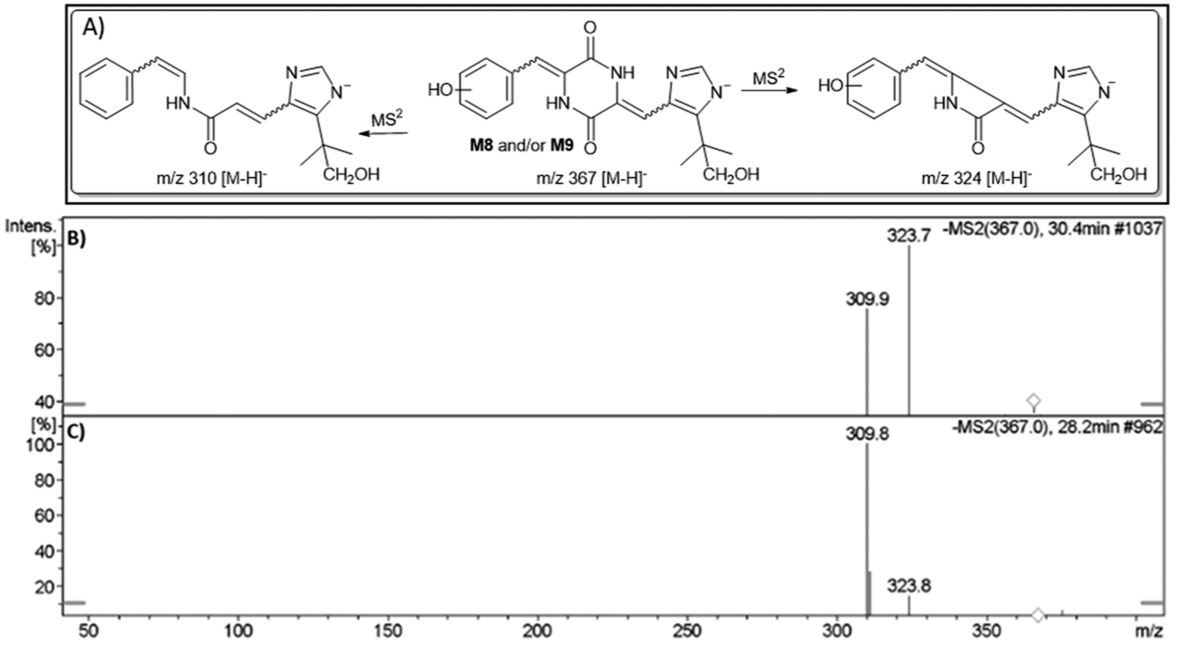

Figure 6. (A) Proposed chemical structure of **M8** and/or **M9** and their most abundant MS/MS fragments; (B) MS/MS spectrum **M8**; (C) MS/MS spectrum of **M9**.

mM ammonium formate in water solvent (A) and acetonitrile solvent (B) were used. At a flow rate of 0.4 mL/min, gradient chromatography (a run of 45 min) was achieved in the water/acetonitrile mixture. 95% of solvent A was used for starting the program, and then within 30 min, solvent B was increased from 5 to 60% and held constant for the next 10 min. The injected sample into the HPLC system was 5 μL.

2.4. Mass Spectrometric Conditions. LC−MS/MS measurements were performed using an Agilent Ion Trap system model 6320 (Agilent Technologies, USA) equipped with an electrospray ionization (ESI) source. ESI was done at RT in the negative mode, the capillary voltage was maintained at 4.5 kV, and the capillary temperature was 325 °C. The scan range was set between 100 and 700 Da. The flow rate of the drying gas (N_2) was 10 L/min. The nebulizer pressure was at 50 psi. Flow injection analysis was used to measure mass spectrometric parameter optimization to attain the highest ion intensity.

3. RESULTS AND DISCUSSION

3.1. LC−MS and LC−MS/MS Analysis of Plinabulin (1). For determination of the possible molecular weights of metabolites of **1**, two possible plans were utilized.[7] In the first one, the possible metabolite structures were hypothesized in light of the metabolism rules of the compounds with similar

https://doi.org/10.1021/acsomega.2c00929
ACS Omega 2022, 7, 21465−21472

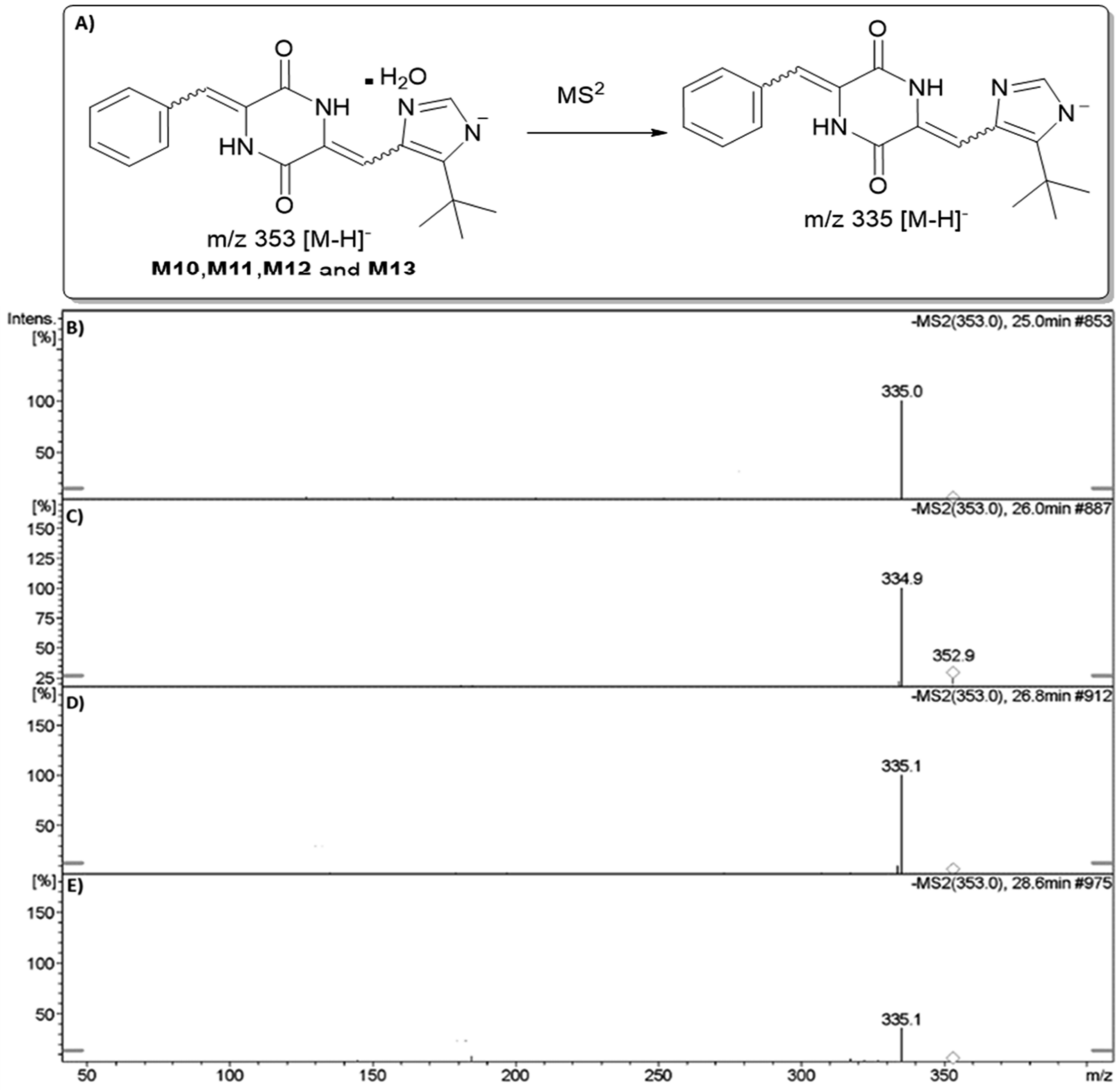

Figure 7. (A) Proposed chemical structure of **M10**, **M11**, **M12**, and **M13** and their most abundant fragments; (B) MS/MS spectrum of **M10**; (C) MS/MS spectrum of **M11**; (D) MS/MS spectrum of **M12**; (E) MS/MS spectrum of **M13**.

structures. Then, in the full-scan mass spectrum, the corresponding peaks of potential metabolites were identified by comparing the chromatographic peaks of the blank samples with those of the drug-treated samples. In the second strategy, MS fragmentation behaviors of the parent compound and its potential metabolites were investigated. Another LC−MS/MS screening was performed by constant neutral loss scan monitoring for metabolites which lost neutral adducts. Screening of total ion chromatograms of **1** in the HLM incubated mixture showed a prominent peak eluting at ∼34.7 min (Figure 1), with a molecular ion peak at m/z 335 corresponding to compound **1**.

The obtained MS^2 spectra of **1** with LC-ITMS showed that the parent peak $[M - H]^-$ with m/z 335 gave many fragments as explained in Figure 2. In the negative scan mode, plinabulin formed a deprotonated molecule $[M - H]^-$ at m/z 335. As illustrated by Figure 2A, MS^2 scan of **1** gave four major fragments which were predominantly formed by cleavage of the amide group from the piperazine ring and cleavage of the CH_2N_2 side chain from the imidazole ring (Figure 2).

3.2. Identification of Proposed Phase-I Metabolites (M1−M17). *3.2.1. Identification of Stereoisomeric Metabolites **M1** and **M2**.* In addition to the peak that appeared with m/z 335 $[M - H]^-$ at the retention time of 34.7 min. which indicated parent **1**, there are two more peaks (**M1** and **M2**) with m/z 335 $[M - H]^-$ at the retention times of 31.8 and 34.2 min, respectively (Figure 3A). These two peaks demonstrated similar deprotonated molecular ion peaks at m/z 335 $[M - H]^-$ and showed same MS/MS fragment ions indicating their isomerization for **1**. The MS/MS spectra of **M1** and **M2** metabolites gave the most abundant ions at m/z 307, 292, and 265 which were similar to the fragment ions of parent **1** (Figure 3B,C). The presence of the fragment ion at m/z 307 with 28 Da less than the parent drug suggested the loss of the carbonyl group from the piperazine ring. Fragment ion at m/z 292 with 43 Da less than the precursor ion indicated the loss of amide group from the piperazine ring. However, the fragment ion at m/z 265 that lost 70 Da from the parent molecule pointed to the loss of carbonyl group from the piperazine ring and CH_2N_2 side chain from the imidazole ring. Based on these data and a comparison of the retention times on HPLC and mass spectra, we concluded that **M1** and **M2** metabolites had known metabolic transformation (stereoisomer) with each other.[8]

https://doi.org/10.1021/acsomega.2c00929
ACS Omega 2022, 7, 21465−21472

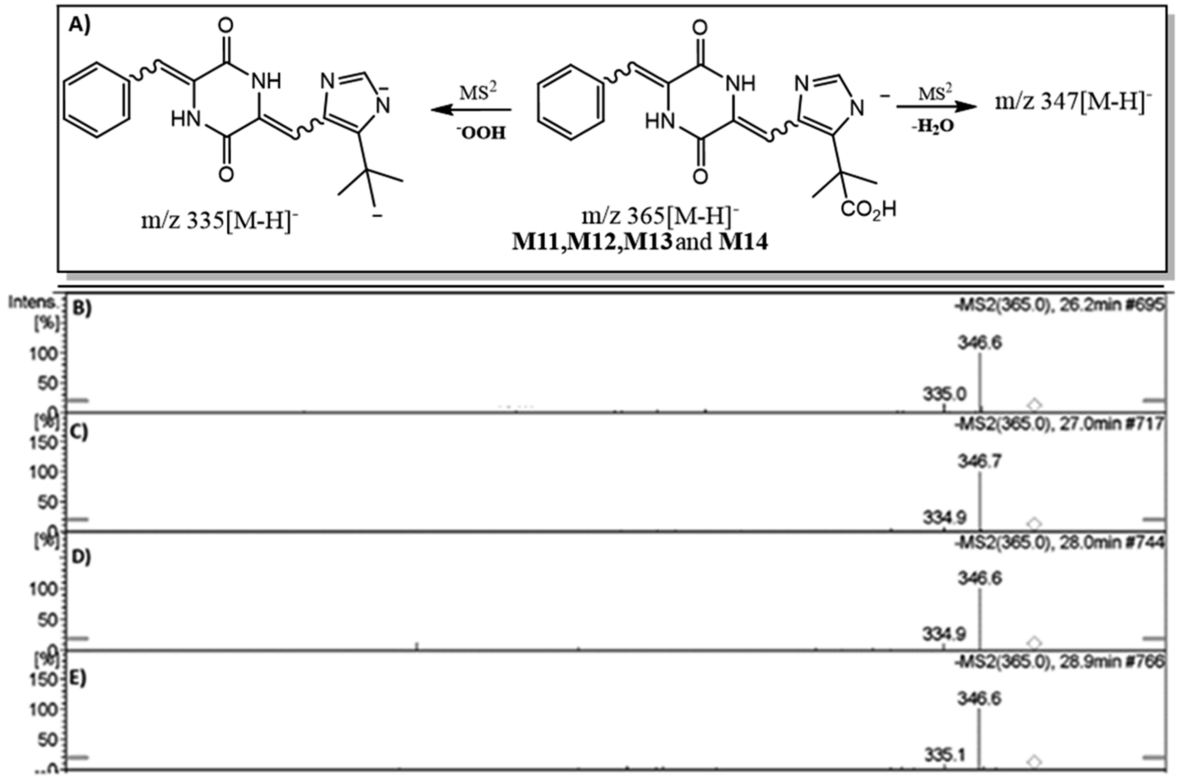

Figure 8. (A) Proposed chemical structure of **M14**, **M15**, **M16**, and **M17** and their most abundant MS/MS fragments; (B) MS/MS spectrum of **M14**; (C) MS/MS spectrum of **M15**; (D) MS/MS spectrum of **M16**; (E) MS/MS spectrum of **M17**.

*3.2.2. Identification of Carbonyl Groups Reduced Metabolites (**M3**–**M5**).* **M3**, **M4**, and **M5** were detected at m/z 337 in a full scan mode with retention times of 39.2, 40.6, and 41.5 min, respectively (Figure 4A). The mass spectrum analysis indicated that the addition of two hydrogens corresponding to the reduced parent **1** most probably occurred.[9]

Upon fragmentation of **M3**, **M4**, and **M5** at $[M - H]^-$ at m/z 337, the MS/MS fragment of m/z 337 gave the most abundant fragment ions with m/z 319 and 301 (Figure 4B–D). The fragment ion (m/z 319) with 18 Da less than the precursor ion indicated the loss of H_2O molecule from the piperazine ring, whereas the fragment ion (m/z 301) with 36 Da less than the precursor ion suggested that two molecules of H_2O are lost. In light of these data, metabolites **M3**–**M5** with m/z 337 were tentatively proposed to be isomers as shown in Figure 4.

*3.2.3. Identification of Hydroxy Metabolites in Aromatic Ring (**M6** and **M7**).* As shown in Figure 5A, **M6** and **M7** were found at the retention times of 28.7 and 29.3 min, respectively, with the deprotonated molecular ion peaks at m/z 351 $[M - H]^-$ in the negative ion mode. Furthermore, **M6** and **M7** gave 16 Da more than **1** suggesting they were monohydroxylated metabolites for **1**.[10]

Fragmentation of both **M6** and **M7** provided the same most abundant fragment ions with m/z 333 and m/z 307 (Figure 5B,C). The product ion at m/z 333 was thought to be formed by the loss of the H_2O molecule (18 Da less than the precursor ion). Fragment ion at m/z 307 with a loss of 44 Da from the precursor ion suggests the loss of hydroxyl group from the benzyl ring and carbonyl group from the piperazine ring. Accordingly, compounds **M6** and **M7** are proposed to be the hydroxylated metabolites of **1**.

*3.2.4. Identification of Hydroxy Together with Reduced Metabolites (**M8** and **M9**).* **M8** and **M9** were detected at m/z 367 $[M - H]^-$ in full scan mode with retention times of 28.2 and 30.4 min, respectively (Figure 6A). The presence of $[M-H]^-$ ions at m/z 367 suggested that both **M8** and **M9** mass values (32 Da) were higher than that of **1**, indicating that these two proposed metabolites are double-hydroxylated metabolites of **1**.

In the MS^2 spectra of **M8**, the presence of the characteristic ions at m/z 324 and 310, which were as the same as those of **M9**, suggested that both metabolites are thought to be isomers (Figure 6B,C). The fragment ion at m/z 324 with 43 Da lower than the precursor ion indicated the loss of amide group from the piperazine ring, while the fragment ion at m/z 310 with 57 Da lower than the precursor ion suggested the loss of amide group from the piperazine ring and hydroxyl group either from the aromatic ring or from the aliphatic chain.

*3.2.5. Identification of Hydrated Metabolites **M10**–**M13**.* The metabolites **M10**, **M11**, **M12**, and **M13** eluted at the retention times of 25, 26, 26.8, and 28.6 min, respectively (Figure 7A), showed the same deprotonated molecular ion peaks at m/z 353 $[M - H]^-$ with18 Da higher than that of m/z 335, suggesting that the molecule of H_2O has attached on the parent drug.[11]

The most abundant fragment ion showed by **M10**-**M13** appeared at m/z 335 with18 Da lower than the precursor ion (Figure 7B–E), suggesting that this fragment ion might be parent **1**. Depending on the obtained data, the four metabolites, namely, **M10**, **M11**, **M12**, and **M13** are proposed to be isomers of hydrated **1**.

*3.2.6. Identification of Oxidized Metabolites (**M14**–**M17**).* The metabolites **M14**–**M17** that eluted at 26.2, 27, 28, and 28.9 min, respectively, displayed deprotonated molecular ion peaks at $[M - H]^-$ at m/z 365, with 30 Da higher than **1**, suggested to be the carboxylic acid metabolites of **1**[12] (Figure 8A).

https://doi.org/10.1021/acsomega.2c00929
ACS Omega 2022, 7, 21465−21472

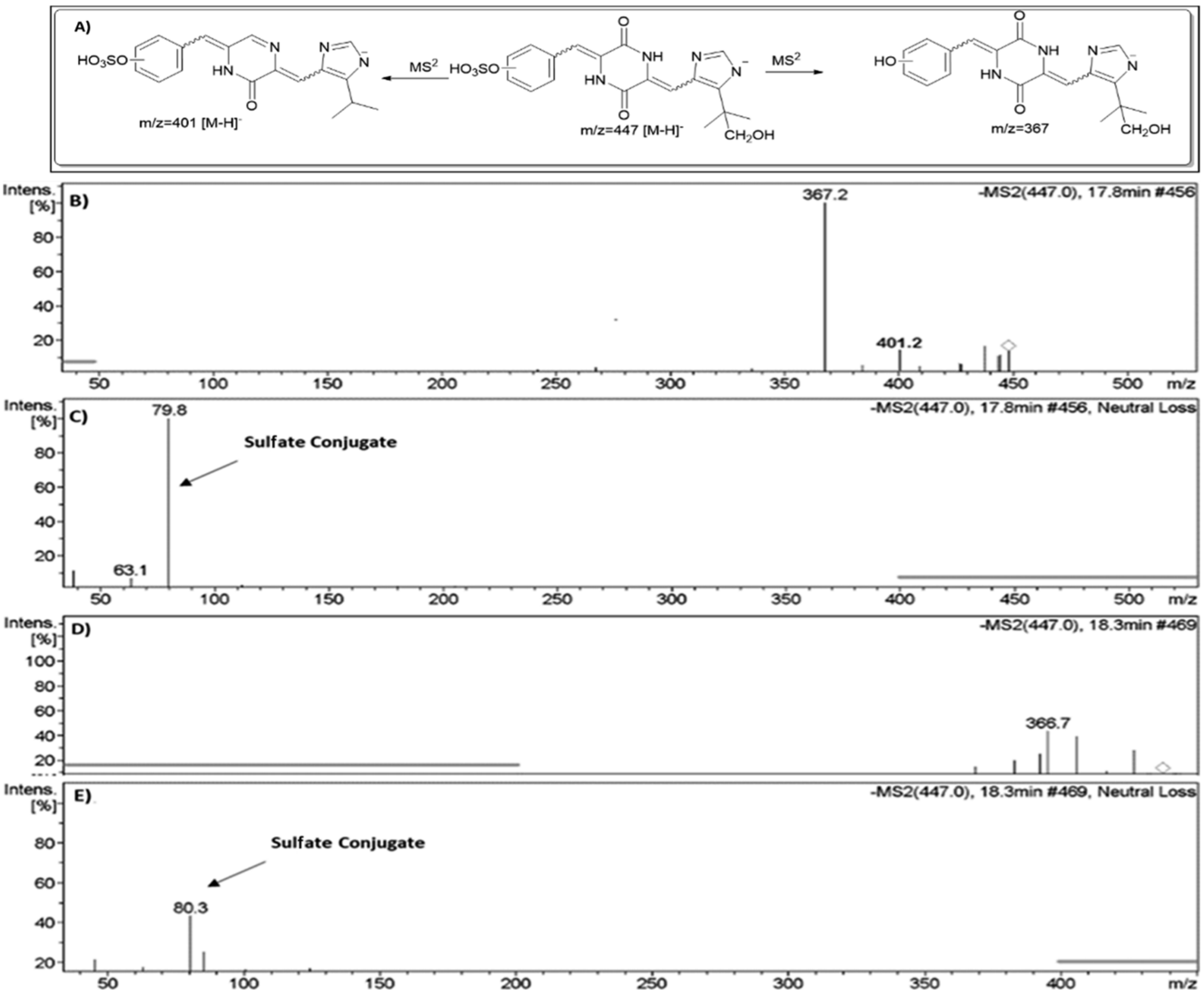

Figure 9. (A) Proposed chemical structure of **M18** and **M19** and their most abundant fragments; (B) MS/MS spectrum of **M18**; (C) constant neutral loss scan of **M18**; (D) MS/MS spectrum of **M19**; (E) constant neutral loss scan of **M19**.

The fragmentation of **M14**−**M17**metabolites provided the same MS/MS fragment ions with m/z 347 and 335 (Figure 8B−E). The product with ion (m/z 347) could be formed by losing of the H_2O molecule $[M\text{-}H_2O]^-$ with 18 Da lower than the precursor ion, while the fragment ion at m/z 335 with 30 Da lower than the precursor ion suggested the losing of −OOH atoms from the carboxylic acid group. In view of the above data, the proposed metabolites (**M14**−**M17**) might be isomers.

3.3. Identification of Proposed Phase-II Metabolites. *3.3.1. Identification of Sulfate Conjugates (M18 and M19).* The metabolites **M18** and **M19** eluted at the retention times of 17.8 and 18.3 min, respectively (Figure 9A) showed the same deprotonated molecular ion peaks at m/z 447 $[M-H]^-$ with 80 Da higher than that of the precursor ion with m/z 367, suggesting that these products proposed to be sulfate conjugation metabolites of **M8** and **M9**.[13]

The MS^2 spectra of the proposed metabolites (**M18** and **M19**) showed the same most abundant fragments at m/z 367 and 401 (Figure 9B,D). The fragment ion at m/z 401 suggested the loss of aliphatic CH_2OH group and H_2O molecule. Another LC−MS/MS screening for the sulfate adduct was performed by constant neutral loss scan monitoring of ions that lost 80 Da (Figure 9C,E).[14] As shown in Figure 8C,E, only two ions at retention times of 17.8 and 18.3 min with m/z 447 were detected, suggesting their isomerization character (Table 1).

4. CONCLUSIONS

In this work, 17 phase-I metabolites of **1** were determined and characterized by the LC−MS/MS method. Upon incubation of plinabulin with HLMs via *in vitro* metabolic reactions including isomerization, hydroxylation, hydration, and oxygenation in the presence of a NADPH-generating system, the metabolites of **1** were formed. Upon incubation of **1** with HepaRG Cells Cryopreserved (phase-II), two sulfate conjugates of **1** were detected and characterized by the LC−MS/MS method and constant neutral loss scan. Structures of those metabolites/conjugates were elucidated by comparing the fragmentation behavior study of those metabolites with the parent molecules. In conclusion, this study is an addition to the drug development of potent VDA drug plinabulin.

https://doi.org/10.1021/acsomega.2c00929
ACS Omega 2022, 7, 21465−21472

Table 1. Proposed Metabolites of Plinabulin (1)

entry	mass m/z $[M - H]^-$	most abundant fragment ions (m/z)	retention time (min)	proposed biotransformation
M1	335.15	307, 292, 265	31.8	isomerization
M2	335.15	307, 292, 265	34.2	isomerization
M3	337.7	319, 301, 257	39.2	reduction
M4	337.7	319, 301, 257	40.6	reduction
M5	337.7	319, 301, 257	41.5	reduction
M6	351.15	307, 333	28.7	monhydroxylation
M7	351.15	307, 333	29.3	monohydroxylation
M8	367.14	324, 310	28.2	dihydroxylation
M9	367.14	324, 310	30.4	dihydroxylation
M10	353.16	335	25.0	hydration
M11	353.16	335	26.0	hydration
M12	353.16	335	26.8	hydration
M13	353.16	335	28.6	hydration
M14	365.13	347, 335	26.2	oxidation
M15	365.13	347, 335	27.0	oxidation
M16	365.13	347, 335	28.0	oxidation
M17	365.13	347, 335	28.9	oxidation
M18	447.10	384, 367	17.8	dihydroxylation and sulfate conjugation
M19	447.10	384, 367	18.3	dihydroxylation and sulfate conjugation

AUTHOR INFORMATION

Corresponding Author

Nasser S. Al-Shakliah − *Department of Pharmaceutical Chemistry, College of Pharmacy, King Saud University, Riyadh 11451, Saudi Arabia;* orcid.org/0000-0002-3386-5145; Phone: +966 1146 70237; Email: nassersalem30@yahoo.com; Fax: +966 1146 76 220

Authors

Adnan A. Kadi − *Department of Pharmaceutical Chemistry, College of Pharmacy, King Saud University, Riyadh 11451, Saudi Arabia*

Rashad Al-Salahi − *Department of Pharmaceutical Chemistry, College of Pharmacy, King Saud University, Riyadh 11451, Saudi Arabia;* orcid.org/0000-0003-1747-2736

A. F. M. Motiur Rahman − *Department of Pharmaceutical Chemistry, College of Pharmacy, King Saud University, Riyadh 11451, Saudi Arabia;* orcid.org/0000-0002-5807-5625

Complete contact information is available at: https://pubs.acs.org/10.1021/acsomega.2c00929

Notes

The authors declare no competing financial interest.

ACKNOWLEDGMENTS

The authors extend their appreciation to the Researchers Supporting Project, King Saud University, Riyadh, Saudi Arabia, for funding this work through grant no. RSP-2021/353.

REFERENCES

(1) Yamazaki, Y.; Tanaka, K.; Nicholson, B.; Deyanat-Yazdi, G.; Potts, B.; Yoshida, T.; Oda, A.; Kitagawa, T.; Orikasa, S.; Kiso, Y.; Yasui, H.; Akamatsu, M.; Chinen, T.; Usui, T.; Shinozaki, Y.; Yakushiji, F.; Miller, B. R.; Neuteboom, S.; Palladino, M.; Kanoh, K.; Lloyd, G. K.; Hayashi, Y. Synthesis and Structure−Activity Relationship Study of Anti-microtubule Agents Phenylahistin Derivatives with a Didehydropiperazine-2,5-Dione Structure. *J. Med. Chem.* **2012**, *55*, 1056−1071.

(2) Ganesher, A.; Chaturvedi, P.; Karkara, B. B.; Chatterjee, I.; Datta, D.; Panda, G. One Pot Synthesis of N-Monoalkylated Plinabulin Derivatives via Multicomponent Protocol and Their Application as Anticancer Agents. *J. Mol. Struct.* **2021**, *1229*, 129830.

(3) Plinabulin Plus G-CSF Earn Priority Review From FDA for CIN. https://www.cancernetwork.com/view/plinabulin-plus-g-csf-earn-priority-review-from-fda-for-cin (accessed Feb 11, 2021).

(4) Millward, M.; Mainwaring, P.; Mita, A.; Federico, K.; Lloyd, G. K.; Reddinger, N.; Nawrocki, S.; Mita, M.; Spear, M. A. Phase 1 Study of the Novel Vascular Disrupting Agent Plinabulin (NPI-2358) and Docetaxel. *Invest. New Drugs* **2012**, *30*, 1065−1073.

(5) Parkin, D. M.; Bray, F.; Ferlay, J.; Pisani, P. Estimating the World Cancer Burden: Globocan 2000. *Int. J. Cancer* **2001**, *94*, 153−156.

(6) Salim, E. I.; Jazieh, A. R.; Moore, M. A. Lung Cancer Incidence in the Arab League Countries: Risk Factors and Control. *Asian Pac. J. Cancer Prev.* **2011**, *12*, 17−34.

(7) Prakash, C.; Shaffer, C. L.; Nedderman, A. Analytical Strategies for Identifying Drug Metabolites. *Mass Spectrom. Rev.* **2007**, *26*, 340−369.

(8) Williams, M. L.; Lennard, M. S.; Martin, I. J.; Tucker, G. T. Interindividual Variation in the Isomerization of 4-Hydroxytamoxifen by Human Liver Microsomes: Involvement of Cytochromes P450. *Carcinogenesis* **1994**, *15*, 2733−2738.

(9) Xie, C.; Zhou, J.; Guo, Z.; Diao, X.; Gao, Z.; Zhong, D.; Jiang, H.; Zhang, L.; Chen, X. Metabolism and Bioactivation of Famitinib, a Novel Inhibitor of Receptor Tyrosine Kinase, in Cancer Patients. *Br. J. Pharmacol.* **2013**, *168*, 1687−1706.

(10) Zhang, J. Y.; Yuan, J. J.; Wang, Y.-F.; Bible, R. H.; Breau, A. P. Pharmacokinetics and Metabolism of a COX-2 Inhibitor, Valdecoxib, in Mice. *Drug Metab. Dispos.* **2003**, *31*, 491−501.

(11) Xiong, A.; Yang, L.; He, Y.; Zhang, F.; Wang, J.; Han, H.; Wang, C.; Bligh, S. W. A.; Wang, Z. Identification of Metabolites of Adonifoline, a Hepatotoxic Pyrrolizidine Alkaloid, by Liquid Chromatography/Tandem and High-Resolution Mass Spectrometry. *Rapid Commun. Mass Spectrom.* **2009**, *23*, 3907−3916.

(12) Sica, D. A.; Gehr, T. W. B.; Ghosh, S. Clinical Pharmacokinetics of Losartan. *Clin. Pharmacokinet.* **2005**, *44*, 797−814.

(13) Levsen, K.; Schiebel, H.-M.; Behnke, B.; Dötzer, R.; Dreher, W.; Elend, M.; Thiele, H. Structure Elucidation of Phase II Metabolites by Tandem Mass Spectrometry: An Overview. *J. Chromatogr. A* **2005**, *1067*, 55−72.

(14) Lafaye, A.; Junot, C.; Ramounet-Le Gall, B.; Fritsch, P.; Ezan, E.; Tabet, J.-C. Profiling of Sulfoconjugates in Urine by Using Precursor Ion and Neutral Loss Scans in Tandem Mass Spectrometry. Application to the Investigation of Heavy Metal Toxicity in Rats. *J. Mass Spectrom.* **2004**, *39*, 655−664.